Chapter 14

Some Monte Carlo Simulations on Nanoparticle Reinforcement of Elastomers

J. E. Mark, T. Z. Sen, A. Kloczkowski

14.1. Introduction

In spite of its great fundamental interest and commercial importance, one of the most important unsolved problems in the area of elastomers and rubberlike elasticity is the lack of a good molecular understanding of the reinforcement provided by fillers such as carbon black and silica [1–5]. More specifically, the reinforcement of elastomers is an interesting aspect in the basic research of nanocomposites in general, and is of much practical importance since the improvements in properties fillers provide are critically important with regard to the utilization of elastomers in almost all commercially significant applications. Some of the work on this problem has involved analytical theory [6–12], but most of it is based on a variety of computer simulations [13–46].

In this context, the present review describes one way in which computational modeling has been used to elucidate the structures and properties of elastomeric polymer networks. One of the main goals has been to provide guidance on how to optimize the mechanical properties of an elastomer, in the present case by the incorporation of reinforcing fillers.

In the present approach, the simulations focus on the ways the filler particles change the distribution of the end-to-end vectors of the polymer chains making up the elastomeric network, from the fact that the filler excludes the chains from the volumes it occupies. The changes in the polymer chain distributions from this filler "excluded volume effect" then cause associated changes in the mechanical properties of the elastomer host matrix. Single polymer chains are

modeled, in the standard rotational isomeric state representation [47–49], and Monte Carlo techniques are used to generate their trajectories in the vicinities of collections of filler particles. A brief overview of the approach is given in the following Section.

14.2. Description of simulations

14.2.1. *Rotational isomeric state theory for conformation-dependent properties*

In rotational isomeric state models, the continuum of rotations occurring about skeletal bonds is replaced by a small number (generally three) of rotational states that are judiciously chosen. Preferences among these states are then characterized by Boltzmann factors as statistical weights, with the required energies obtained by either potential energy calculations or by interpreting available conformation-dependent properties in terms of the models. Multiplication of matrices containing these statistical weights is then used to generate the partition function and related thermodynamic quantities, and multiplications of similar matrices containing structural information are then used to predict or interpret various properties of the chains [47–49]. Examples of such properties are end-to-end distances, radii of gyration, dipole moments, optical anisotropies, *etc.* as unperturbed by intramolecular excluded volume interactions between chain segments [50].

14.2.2. *Distribution functions*

The extension of these ideas most relevant in the present context is the use of this model to generate *distributions* of end-to-end distances, instead of simply their averages [51]. The same statistical weights were used in Monte Carlo simulations to generate representative chains, and their end-to-end distances, r, were calculated. The corresponding distribution function was obtained by accumulating large numbers of these Monte Carlo chains with end-to-end vectors within various space intervals, and dividing these numbers by the total number of the chains, N. The distances were then placed into a histogram to produce the desired end-to-end vector probability distribution function, $P(r)$ or $P(r/nl_0)$, where n is the number of skeletal bonds of length l_0. The histogram generally consisted of 20 equally spaced intervals over the allowed range $0<(r/nl_0)<1$, since previous studies showed that this choice was the most suitable for obtaining probability distribution functions [52]. The function $P(r/nl_0)$ was smoothed using the IMSL (International Mathematics and Statistics Library) cubic spline subroutine CSINT (Cubic Spline INTerpolant). The smoothing procedure is necessary for the proper calculation of the stress-strain isotherms from the Monte Carlo histogram [52].

These distributions are very useful for chains that cannot be described by the Gaussian limit, specifically chains that are too short, too stiff, or stretched too close to the limits of their extensibility [51]. In particular, they have

documented how inadequate the Gaussian distribution is for short chains of polyethylene and poly(dimethylsiloxane) (PDMS) particularly in the region of high extension that is critical to an understanding of ultimate properties.

14.2.3. *Applications to unfilled elastomers*

The present application of these calculated distribution functions is the prediction of elastomeric properties of the chains within the framework of the Mark-Curro theory [51,53] described below.

The distribution, $P(r)$, of the end-to-end vectors, r, is directly related to the Helmholtz free energy, $A(r)$, of a chain by

$$A(r) = \mathrm{c} - \mathrm{kT} \ln P(r), \tag{14.1}$$

where c is a constant. The resulting perturbed distributions are then used in the "three-chain" elasticity model [54] to obtain the desired stress-strain isotherms in elongation. For the specific case of this model, the general expression for ΔA takes the form

$$\Delta A = \frac{\nu}{3}\left[A(r_0\alpha) + 2A(r_0\alpha^{-\frac{1}{2}}) - 3A(r_0)\right] \tag{14.2}$$

for elongations that are "affine" (in which the molecular deformations parallel the macroscopic deformation in a linear manner). Here, α is the elongation ratio L/L_i, ν is the number of chains in the network, and r_0 is the value of root-mean-square end-to-end distance of the undeformed network chains.

One quantity of primary interest here is the nominal or engineering stress, f^*, defined as the elastic force at equilibrium per unit cross-sectional area of the sample in the undeformed state:

$$f^* = -T\left(\frac{\partial \Delta A}{\partial \alpha}\right)_T. \tag{14.3}$$

Substitution of Eq. 14.2 into Eq. 14.3 then gives

$$f^* = -\frac{\nu \mathrm{k} T r_0}{3}\left[G'(r_0\alpha) - \alpha^{-\frac{3}{2}} G'(r_0\alpha^{-\frac{1}{2}})\right] \tag{14.4}$$

where $G(r) = \ln P(r)$, and $G'(r)$ denotes the derivative dG/dr. The modulus (or "reduced stress") is defined by $[f^*] \equiv f^*/(\alpha - \alpha^{-2})$ and is often fitted to the Mooney-Rivlin semi-empirical formula $[f^*] \equiv 2\mathrm{C}_1 + 2\mathrm{C}_2\alpha^{-1}$ [54–56], where C_1 and C_2 are constants independent of deformation α.

Such results are often shown as Mooney-Rivlin plots [51], in which the calculated values of the reduced stress or modulus normalized by the value given by the Gaussian limit are shown as a function of reciprocal elongation. In a test case, the value of unity was obtained for long chains, in this case those having $n = 250$ skeletal bonds, as expected. In the case of shorter chains (having $n =$ 20 or 40 skeletal bonds) there were upturns in modulus with increasing elongation that were similar to those shown in bimodal networks in which short chains

are introduced to give advantageous increases in ultimate strength and modulus [57–59].

14.2.4. *Applications to filled elastomers*

In this case, the same Monte Carlo simulations were carried out as was done for the unfilled networks, but now each bond of the chain was tested for overlapping with a filler particle as the chain was being generated [28]. If any bond penetrated a particle surface, the entire chain conformation was rejected and a new chain started. Some specific illustrative examples of such investigations are given below.

14.3. Spherical particles

14.3.1. *Particle sizes, shapes, concentrations, and arrangements*

The particle sizes of greatest interest are those used commercially, with small particles giving significantly better reinforcement than larger ones. The primary particles are generally assumed to be spherical. The concentrations or "loadings" in the simulations are generally relatively small, smaller than those used commercially, since larger concentrations lead to unacceptably high attritions from chains running into particles. In actual filled elastomers, the particles are dispersed at least relatively randomly, but it is of interest to do simulations on regular particle arrangements as well [28].

14.3.1.1. *Regular arrangements, on a cubic lattice*

In these simulations, a filled PDMS network was modeled as a composite of cross-linked polymer chains and spherical filler particles arranged in a regular array on a cubic lattice [14,40]. The arrangement is shown schematically in Figure 14.1. The filler particles were found to increase the non-Gaussian behavior of the chains and to increase the moduli, as expected. It is interesting to note that composites with such structural regularity have actually been produced [60,61], and some of their mechanical properties have been reported [62,63].

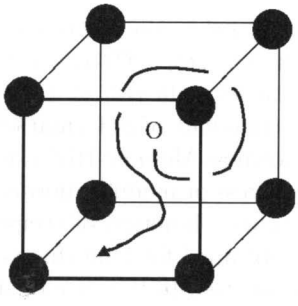

Figure 14.1. Schematic view of a polymer chain being generated within a series of filler particles in cubic arrangements

14.3.1.2. *Random arrangements, within a sphere*

In a subsequent study [16], the reinforcing particles were randomly distributed, as is illustrated in Figure 14.2. The system was taken to be a sphere having a radius equal to the end-to-end distance of the completely stretched out chain. The chain being generated was started at the center of the sphere, and this was the only place a filler particle could not be placed. Otherwise, the particles required to give the desired loading were randomly dispersed over the sample volume shown.

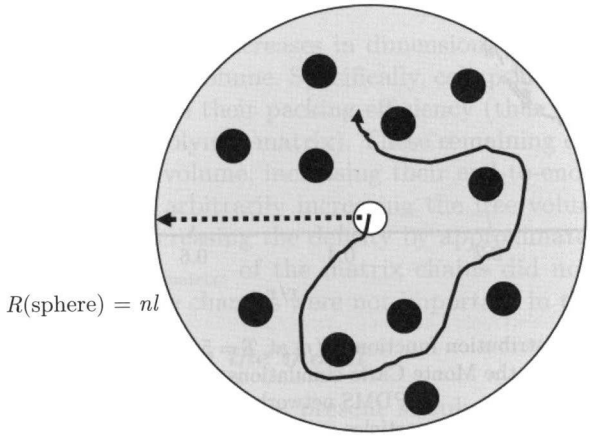

Figure 14.2. Schematic view of a polymer chain and randomly-distributed filler particles. The origin of the chain was placed at the center of the sphere of radius $R(\text{sphere}) = nl$ (maximum extension, r_{max}). All the filler particles were placed randomly in non-overlapping arrangements within the sphere, except of course at its center (where the chain started its trajectory). Chain conformations that trespassed on any particle were rejected, and statistical calculations were performed on the remaining, acceptable conformations

14.3.2. *Distributions of chain end-to-end distances*

Of greatest interest here is whether the particles cause increases or decreases in the end-to-end distances, with this expected to depend particularly on the size of the filler particles, but presumably on other variables such as their concentration in the elastomeric matrix as well.

14.3.2.1. *Typical results*

Some illustrative results for filler particles within a PDMS matrix are described in Figure 14.3 [16,40]. One effect of the particles was to increase the dimensions of the chains, in the case of filler particles that were small relative to the dimensions of the network chains. In contrast, particles that were relatively large tended to decrease the chain dimensions. Since these changes in dimensions arising from the filler excluded volume effects are of critical importance, it is necessary to put them into a larger context.

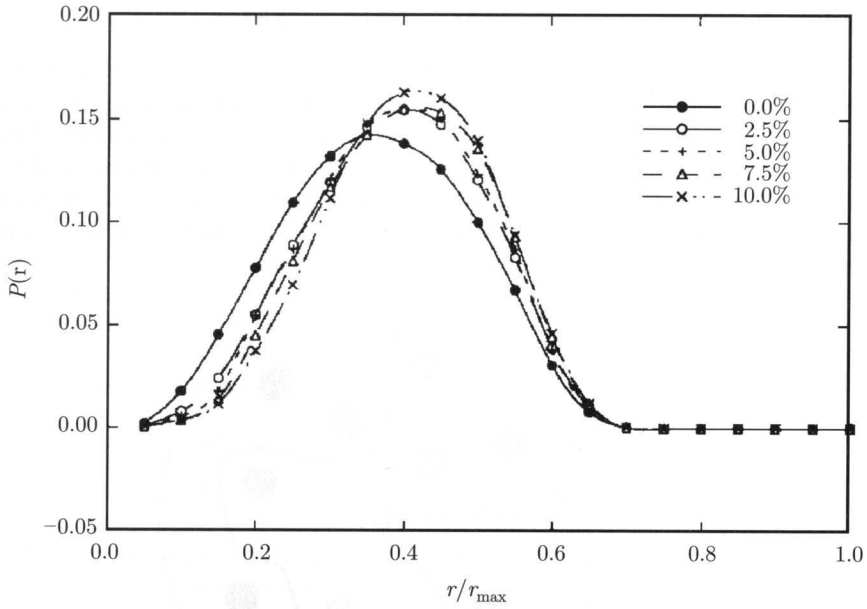

Figure 14.3. Radial distribution functions $P(r)$ at $T = 500$ K for network chain end-to-end distances obtained from the Monte Carlo simulations. The results are shown as a function of the relative extension, r/r_{max}, for PDMS networks having 50 skeletal bonds between cross links [16]. The radius of the filler particles was 5 Å, and the values of the volume % of filler present are indicated in the inset

14.3.2.2. *Relevant neutron scattering results*

These simulation results on the distributions are in agreement with some subsequent neutron scattering experiments on deuterated and non-deuterated chains of PDMS [64,65]. The polymers contained silica particles that were surface treated to make them inert to the polymer chains, as was implicitly assumed in the simulations. These experimental results also indicated chain extensions when the particles were relatively small, and chain compressions when they were relatively large. Increases in chain dimensions have also been recently reported in scattering studies on heavily cross-linked polystyrene (PS) spheres introduced as filler particles into a PS matrix [66].

14.3.2.3. *Comparisons with some related simulations*

Some recent dynamic Monte Carlo simulations have also reported increases in chain dimensions in filled systems [67]. There have been several reports of simulations, however, that have yielded results in disagreement with the described simulations and the two corresponding scattering reports mentioned above. The major difference in approach was the use of dense collections of chains instead of single chains sequentially generated in the vicinities of the filler

particles. Specifically, the simulations by Vacatello [18,38] and by Kumar *et al.* [39] find chain dimensions that are either unchanged by the filler particles or are decreased.

In a rather different type of simulation, Mattice *et al.* [68] generated particles within a matrix by collapsing some of the chains into domains that would act as reinforcing filler. They found that small particles did lead to significant increases in chain dimensions, while large particles led to moderate decreases, in agreement with the single-chain simulations and scattering experiments. These simulations parallel the already cited experimental scattering study of PS spheres in a PS matrix [66].

It was suggested that the increases in dimensions could have come from inadvertent increases in free volume. Specifically, collapsing some of the chains into particles could decrease their packing efficiency (thus increasing the free volume of the remaining polymer matrix). These remaining chains could then expand into the new free volume, increasing their end-to-end distances. This possibility was tested by arbitrarily increasing the free volume (at constant numbers of chains) by decreasing the density by approximately 4% [69]. The mean-square radii, $<s^2>_{\text{matrix}}$, of the matrix chains did not change at all, indicating that free volume changes were not important in this context.

14.3.2.4. *Improvements in the model*

Because of these discrepancies, the present simulations were refined in an attempt to understand the differences described [35]. This involved (i) relocating the particles periodically during a simulation, (ii) starting the chains at different locations, (iii) using Euler matrices to change the orientations of the chains being generated, and (iv) replacing the "united atom" approach by detailed atom specifications. None of these modifications significantly changed the results obtained. An additional modification, generating dense collections of chains, is in progress [70].

14.3.2.5. *Distributions of particle diameters*

Also in progress are simulations to determine any effects of having multimodal distributions of particle sizes [71]. Looking at this issue was encouraged by the improvements in properties obtained by using bimodal distributions of network chain lengths in elastomers [58] and thermosets [72], and bimodal distributions of the diameters of rubbery domains introduced into some thermoplastics [73–75].

14.3.3. *Stress-strain isotherms*

There are two items of primary interest here, specifically increases in modulus in general, and upturns in the modulus with increasing deformation. Results are typically expressed as the reduced nominal or engineering stress as a function of deformation. The area under such curves up to the rupture point of the sample then gives the energy of rupture, which is the standard measure of the toughness of a material [57].

14.3.3.1. *Typical results*

Figure 14.4 shows the stress-strain isotherms in elongation [16] corresponding to the distributions shown in Figure 14.3. There are substantial increases in modulus that increase with increase in filler loading, as expected. Additional increases would be expected by taking into account other mechanisms for reinforcement such as physisorption, chemisorption, *etc.*, as described below. Similar studies can be found elsewhere [41–46].

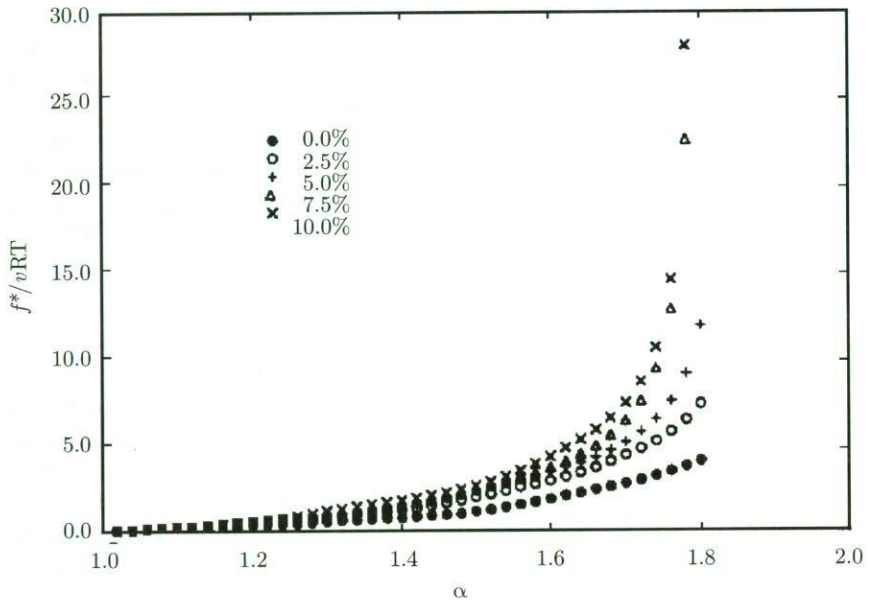

Figure 14.4. Normalized stresses calculated from the distributions shown in Figure 14.3

14.3.4. *Effects of arbitrary changes in the distributions*

One additional interesting result is the observation that in some cases, chain compression can also cause increases in modulus. This is being clarified by making some arbitrary changes in the distributions obtained and documenting the effects these changes have on the corresponding simulated stress-strain isotherms. For example, the curves can be shifted to lower and higher values of the chain dimensions, as is illustrated by two of the curves in Figure 14.5 [40]. The "fitted curve" is produced as follows: the distribution of end-to-end distances for the 500,000 Monte Carlo polyethylene chains of 50 bonds at 550 K is fitted to a Gaussian curve and this curve is called "fitted". Then this curve is shifted in different directions mathematically to obtain other representative curves called left-shifted, right-shifted, and up-shifted.

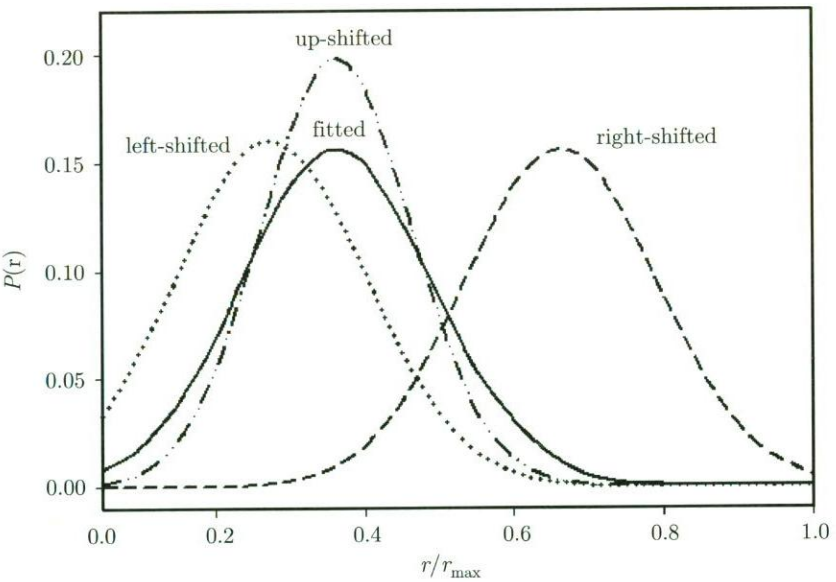

Figure 14.5. Arbitrary illustrative shifts in end-to-end distance distributions, to smaller and larger values of r. Also shown is an arbitrary illustrative narrowing of an end-to-end distance distribution, at the same most-probable value of r

This gives the isotherms shown in Figure 14.6, which show the expected increases in modulus when the chains are extended by the filler excluded volume

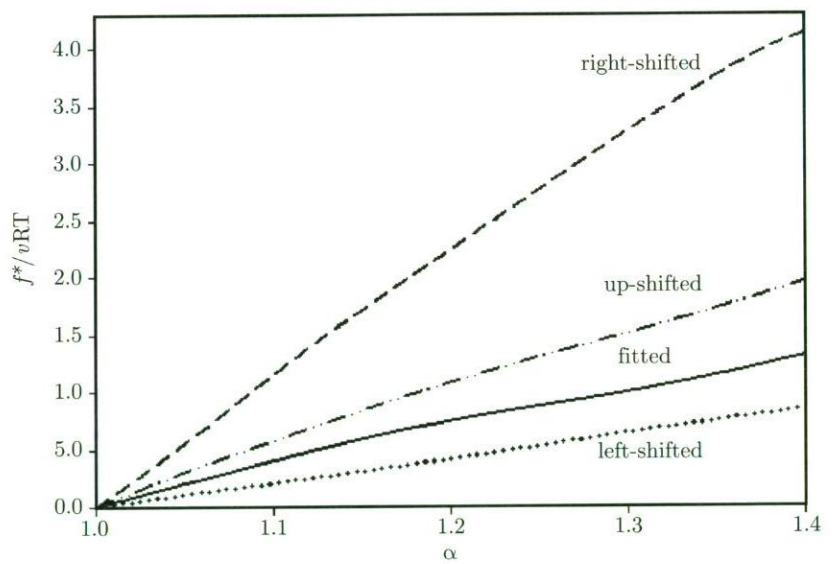

Figure 14.6. Normalized stresses calculated for the distribution shifts shown in Figure 14.5

effect, and decreases when the chains are compressed. Unexpected results are obtained, however, when the distribution is narrowed at the same most-probable value of the chain dimensions, as illustrated in Figure 14.5 [40]. The narrowing causes the peak defining the most-probable value to shift upward to keep the area under the curve the same, as is required. In this case, the change in the shape of the distribution does indeed cause an increase in the modulus, as shown in Figure 14.6. This is consistent with other simulations finding increases in modulus even when the chains are compressed, since it demonstrates that the mechanical properties can depend on subtle features of the distribution, beyond merely some average value of the chain dimensions!

14.3.5. *Some preliminary results on physisorption*

Preliminary studies have been carried out to model the effects of physical adsorption of some of the chains onto the particle surfaces [70]. The goal was to determine the relative importance of the two major effects expected. These are the increase in the effective number of chains or cross links (which would certainly increase the elastic force, stress, and modulus), and the changes in the end-to-end distances of the chains that are adsorbed (which could conceivably either increase or decrease these elastomeric properties). Specifically, amorphous PE chains having 50 skeletal bonds were Monte Carlo generated in the presence of filler particles having 20 Å diameters, with the first atom of each chain being attached to the particle surface.

The reference case of "no adsorption" was treated as follows. After the chains were generated, the conformations overlapping the filler were discarded. Over 300,000 chain conformations survived and were kept for subsequent calculations. For the "adsorption" case, any chain being generated that hit the filler surface was assumed to have been adsorbed onto the surface. If the chain could not escape the filler surface because of conformational constraints, then that chain was discarded. Also discarded were chains that did not hit the filler surface at all. Over 50,000 chains survived elimination, and were accepted as "adsorbed" chains.

Every time a chain hit the filler surface, the number x of bonds adsorbed onto the filler surface was taken to be either 1, 2, or 3 (described as 1-bond, 2-bond, and 3-bond adsorption). These bonds were assumed to be adsorbed in such a way that they formed a loop on the filler surface, so that the end-to-end vectors of the adsorbed parts of the chains on the surfaces were zero (even, tentatively, for the 1-bond adsorption case).

The results showed that if a chain had hit the filler surface, it did it 1.7 times per chain on the average. The first interesting difference between the no-adsorption and the adsorption cases is the decrease in end-to-end distances of the adsorbed chains, as is illustrated in Figure 14.7. When adsorption occurred, then the PE should be stretchable to higher elongations before its modulus increased markedly. This is shown in Figure 14.8. Similarly, as is shown in Figure 14.9, the moduli of the adsorbed chains were lower. This suggests the

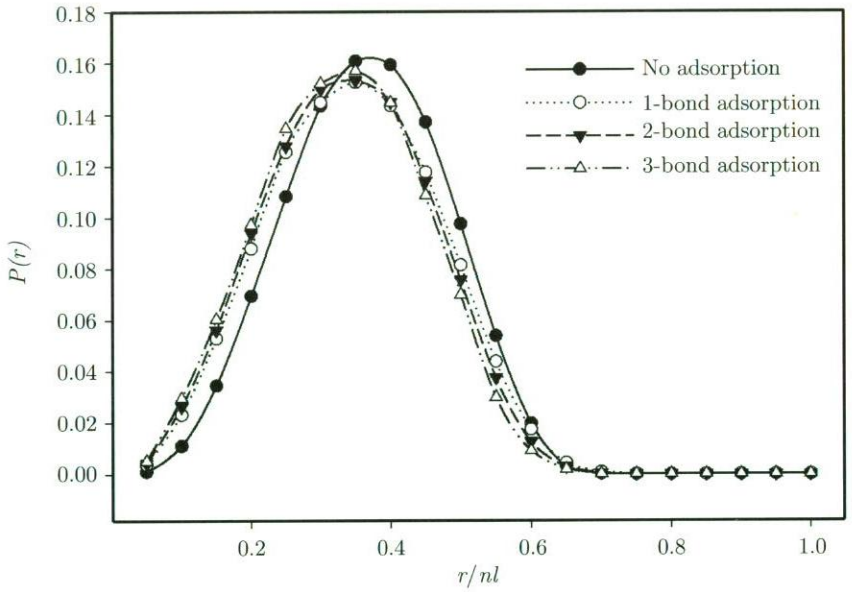

Figure 14.7. The distribution function of the end-to-end distance for PE chains of 50 bonds, with a filler radius of 20 Å at 550 K

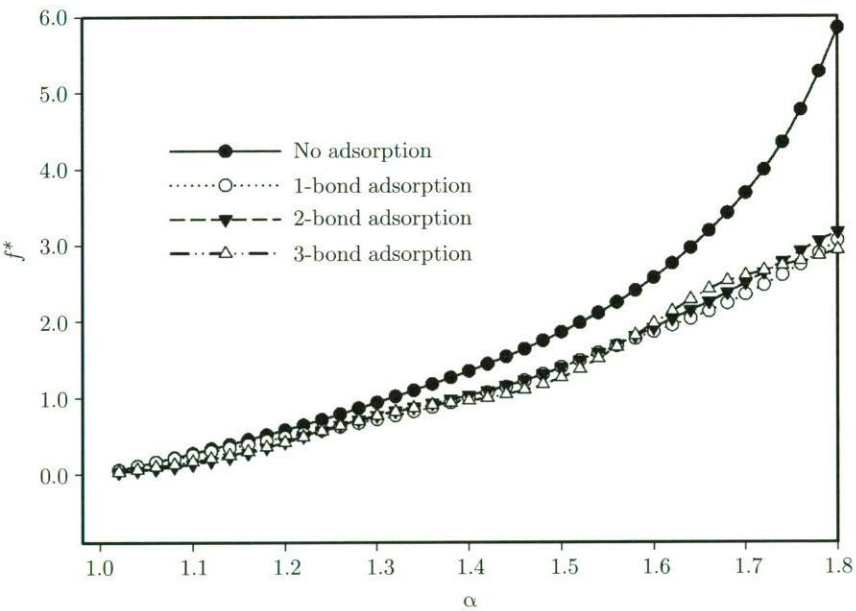

Figure 14.8. Nominal stress, f^*, for PE chains as a function of extension ratio, α, for the PE chains described in Figure 14.7

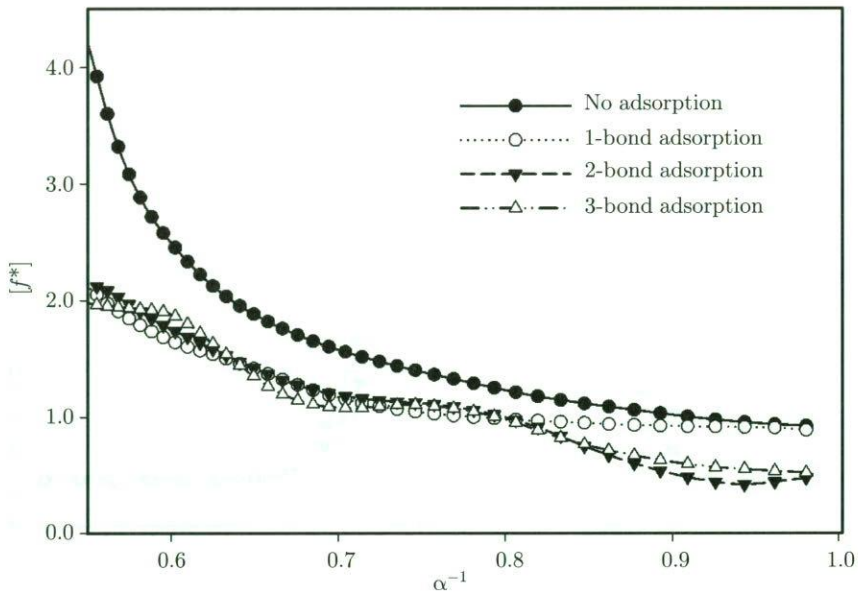

Figure 14.9. Reduced stress $[f^*]$ as a function of α^{-1} for the PE chains described in Figure 14.7

induced changes in chain conformations were less important with regard to these mechanical properties than the increases in the effective number of chains or cross links resulting from the adsorptions.

Calculations performed for a range of temperatures also suggested interesting differences. Specifically, increase in temperature also caused decreases in chain end-to-end distances, as is illustrated in Figure 14.10. This may be due at least in part to the fact that amorphous PE chains shrink upon increase in temperature. More specifically, the temperature coefficient of the unperturbed dimensions is $d\ln\langle r^2\rangle_0/dT = -1.1\times10^{-3}$ deg^{-1} [47–49]. The nominal stress and the reduced stress or modulus decrease correspondingly, as is shown in Figures 14.11 and 14.12, respectively.

14.3.6. *Relevance of cross linking in solution*

The cases where the filler causes compression of the chain are relevant to another area of rubberlike elasticity, specifically the preparation of networks by cross linking in solution followed by removal of the solvent [57]. This is shown schematically in Figure 14.13. Such experiments were initially carried out to obtain elastomers that had fewer entanglements and the success of this approach was supported by the observation that such networks came to elastic equilibrium much more rapidly. They also exhibited stress-strain isotherms in elongation that were closer in form to those expected from the simplest molecular theories of rubberlike elasticity.

In these procedures, the solvent disentangles the chains prior to their cross linking, and its subsequent removal by drying puts the chains into a "super-

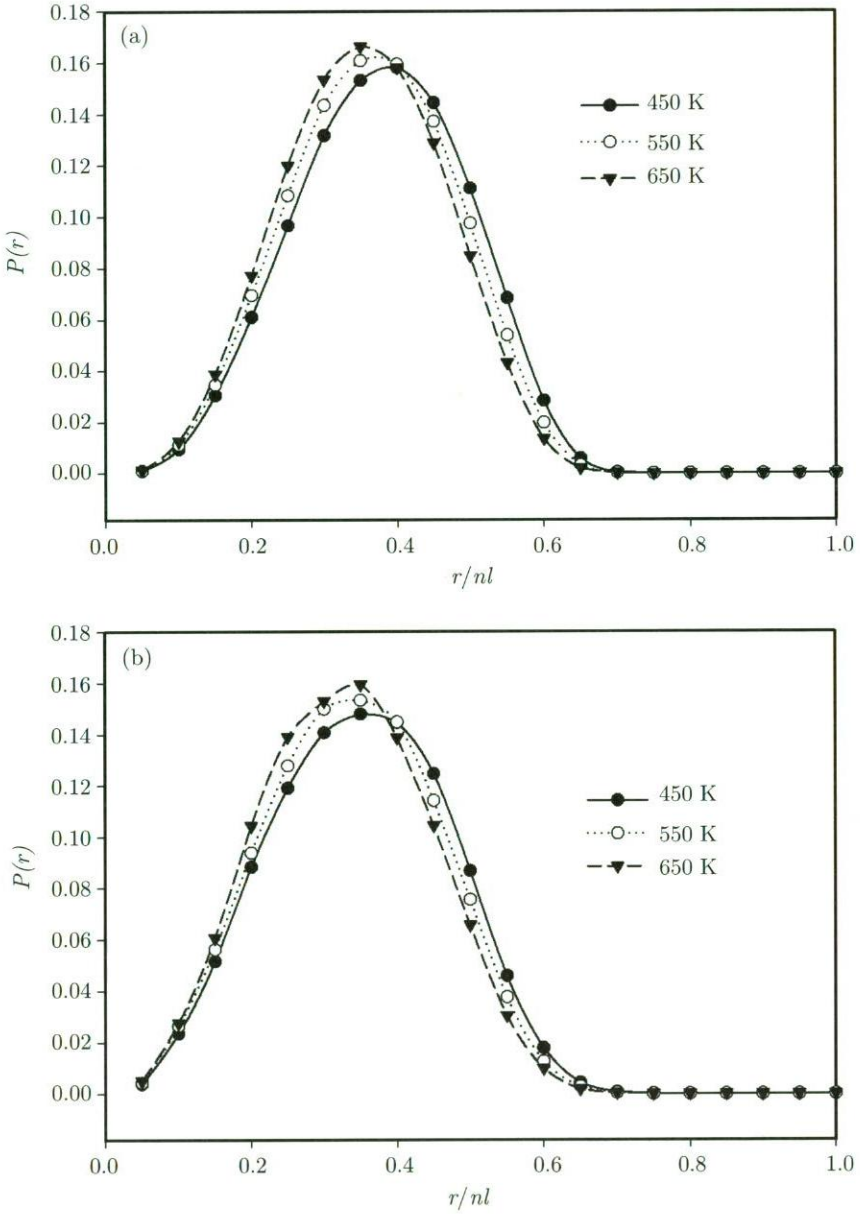

Figure 14.10. The effects of temperature on the distribution function for the end-to-end distances for the PE chains for (a) no adsorption; (b) 2-bond adsorption

contracted" state [57]. Experiments on strain-induced crystallization carried out on such solution cross-linked elastomers indicated that the decreased entangling was less important than the supercontraction of the chains, in that crystalliza-

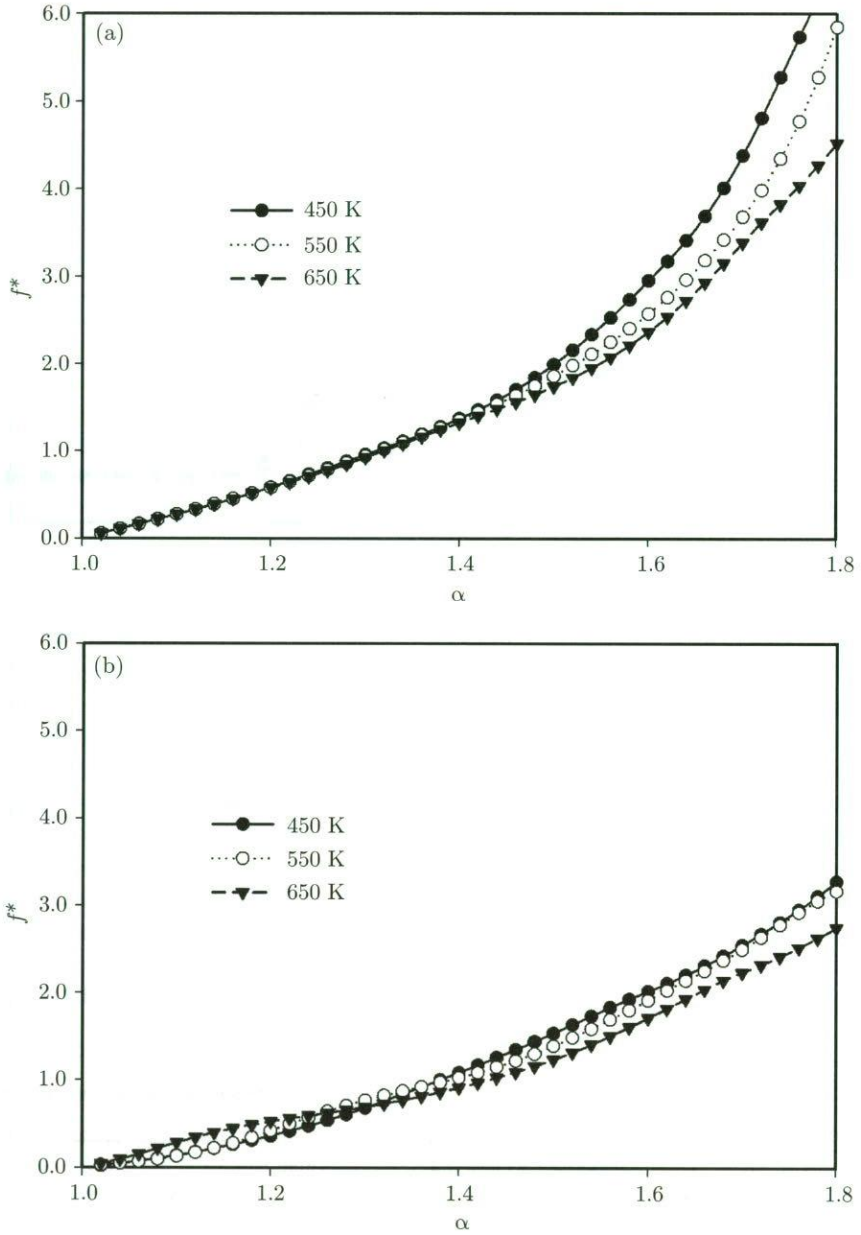

Figure 14.11. The effects of temperature on the nominal stress, f^*, for the PE chains for (a) no adsorption; (b) 2-bond adsorption

tion required larger values of the elongation than was the case for the usual elastomers cross linked in the dry state [76,77]. More recent work in this area has focused on the unusually high extensibilities of such elastomers [78–80].

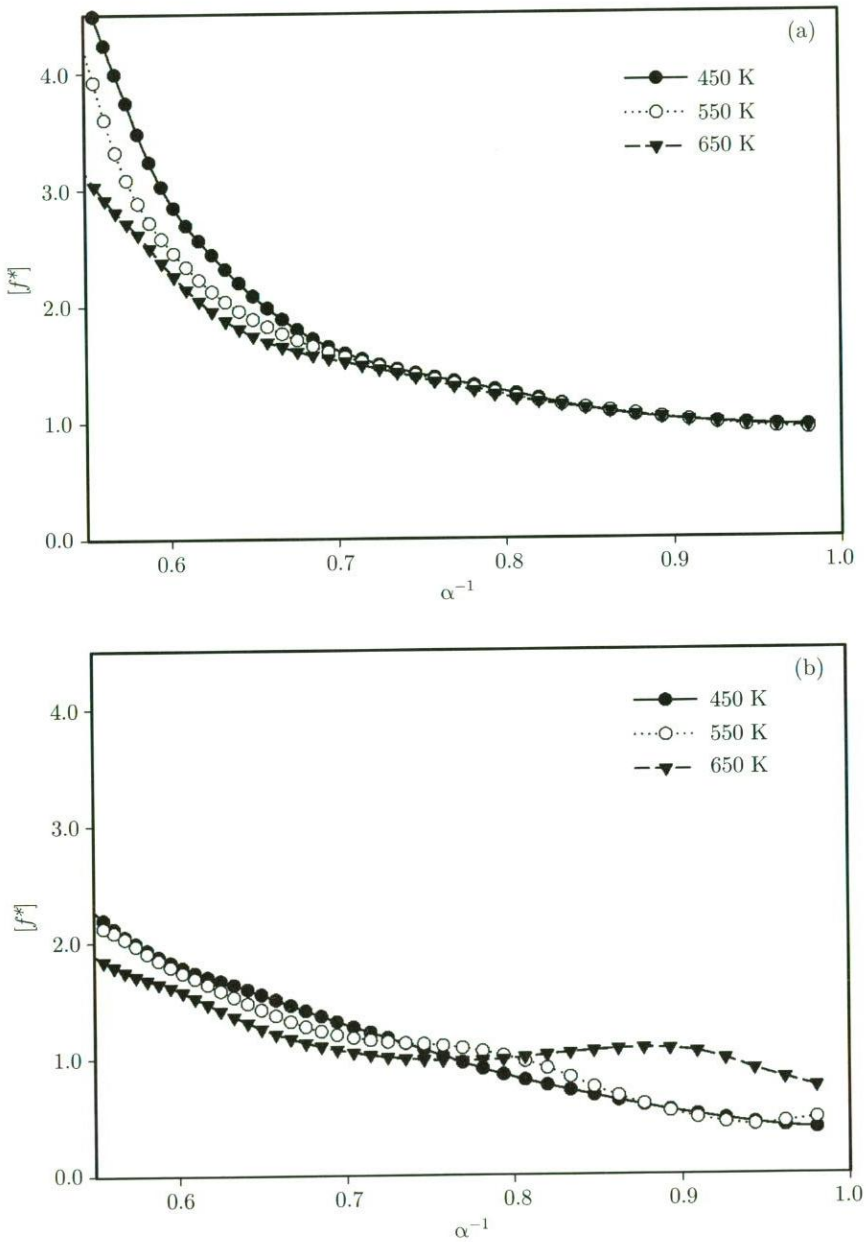

Figure 14.12. The effects of temperature on the reduced stress $[f^*]$ for the PE chains for (a) no adsorption; (b) 2-bond adsorption

In any case, the present simulations should help elucidate molecular aspects of phenomena in this research area as well.

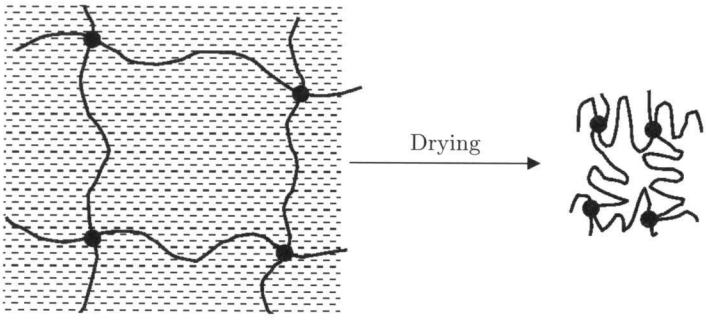

Figure 14.13. Forming a "super-compressed" network by cross linking in solution, followed by drying

14.3.7. *Detailed descriptions of conformational changes during chain extension*

An illustration of this application involves the nominal stress for syndiotactic polypropylene at T = 481 K as a function of elongation for different chain lengths, for a filler radius of 10 Å [40]. The Monte Carlo simulations were performed using recently derived conditional bond probabilities for stereoregular vinyl chains [81].

Some typical results obtained for chains having either 100 or 200 skeletal bonds are shown elsewhere [40]. At the beginning of the elongation, the chains of the two different lengths followed the same linear curve, which corresponds to the elastomeric region. This linearity is consistent with the equation for the deformation of a single chain in which the stress, f^*, is directly proportional to its end-to-end distance, r [82]. Specifically,

$$f^* = (3\mathrm{kT}/<r^2>_0)r \tag{5}$$

where $<r^2>_0$ represents the mean-square unperturbed dimension of the chain.

A "plastic" region (characterized by large increases in stress) appeared at lower elongations for chains having 100 skeletal bonds, as compared with those having 200. Chains of 100 bonds required greater stresses to be elongated once this critical point was reached, and this need for higher stresses can be explained in terms of its end-to-end distance distribution [40]. Since the chains of 100 bonds are already more extended than the chains of 200 bonds, the amount of additional elongation they can endure until the elastic region ends is more limited. Once the plastic region is reached, the stress development showed a non-linear character as the elongation was increased.

14.4. Ellipsoidal particles

14.4.1. *General features*

Non-spherical filler particles are also of considerable interest. Prolate (needle-shaped) particles can be thought of as a bridge between the roughly spherical

particles used to reinforce elastomers [83] and the long fibers frequently used for this purpose in thermoplastics and thermosets [84]. Oblate (disc-shaped) particles can be considered as analogues of the much-studied clay platelets used to reinforce a variety of materials [85–96].

14.4.1.1. *Regular arrangements of prolate ellipsoids*

In one particularly relevant series of experiments, initially spherical particles of polystyrene were deformed into prolate ellipsoids by (i) heating the elastomeric PDMS matrix in which they resided above the glass transition temperature of the PS, (ii) stretching the matrix uniaxially, and then (iii) cooling it under the imposed deformation [97]. The technique is illustrated schematically in Figure 14.14. It is important to note that this approach also orients the axes of the non-elliptical particles, as shown in the top portion of the figure. If desired, the orientation can be removed by dissolving away the host matrix, and then re-dispersing the particles randomly within another polymer that is subsequently cross linked. This is illustrated in the bottom portion of the sketch.

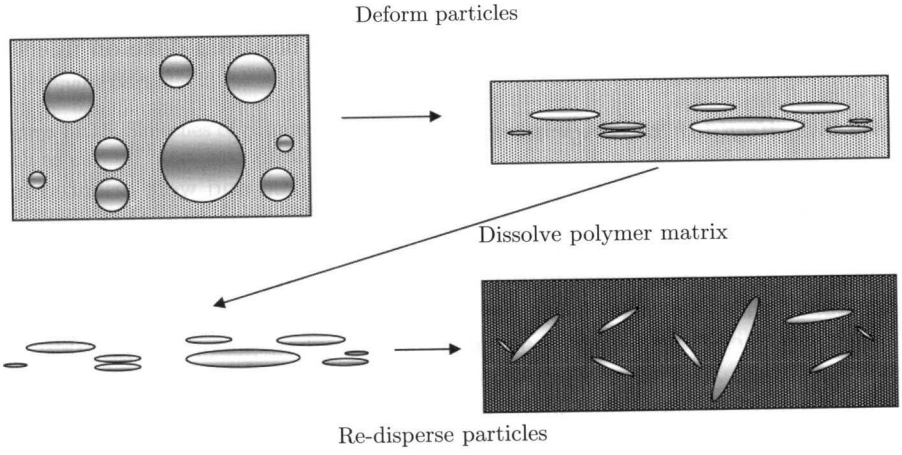

Figure 14.14. Originally spherical filler particles being deformed into prolate (needle-shaped) ellipsoids by stretching a polymer matrix in which they reside. This *in situ* approach also orients the axes of the deformed particles in the direction of the stretching. The orientation can be removed by dissolving away the host polymer matrix and then redispersing the ellisoidal particles isotropically within another polymer (giving reinforcement that is presumably isotropic)

Some relevant simulations [19,42] were presented as the moduli as a function of reciprocal elongation for particles having various values of the radius and loading volume fraction. The anisotropy in structure causes the values of the modulus in the longitudinal direction to be significantly higher than those in the transverse directions.

These simulated results are in at least qualitative agreement with the experimental differences in longitudinal and transverse moduli obtained experimentally [97]. Quantitative comparisons are difficult, in part because of the non-uniform stress fields around the particles after the deforming matrix is allowed to retract.

14.4.1.2. *Randomized arrangements of prolate ellipsoids*

In this case, isotropic behavior is expected, due to the lack of orientation dependence between the non-spherical particles and the deformation axis regardless of the shapes of the particles. The simulated results confirmed this expectation that the reinforcement from randomly-oriented non-spherical filler particles is isotropic regardless of the anisometry of their shapes. There may be difficulties on the experimental side in obtaining completely randomized orientations (and dispersions), because of the tendency of non-spherical particles to order themselves, particularly in the types of flows that accompany processing techniques or even the simple transfers of polymeric materials.

14.4.2. *Oblate ellipsoids*

In spite of their inherent interest, relatively little has been done on fillers of this shape.

14.4.2.1. *Regular arrangements*

The particles were again placed on a cubic lattice [20], and were oriented in a way consistent with their orientation in PS–PDMS composites that were the subject of an experimental investigation [98]. In general, the network chains tended to adopt more compressed configurations relative to those of prolate particles having equivalent sizes and aspect ratios. The elongation moduli were found to depend on the sizes, number, and axial ratios of the particles, as expected. In particular, the reinforcement from the oblate particles was found to be greatest in the plane of the particles, and the changes were in at least qualitative agreement with the corresponding experimental results [98]. In the experimental study, axial ratios were controllable, since they were generally found to be close to the values of the biaxial draw ratio employed in their generation. The moduli of these anisotropic composites were reported, but only in the plane of the biaxial deformation [98]. It was not possible to obtain moduli in the perpendicular direction, owing to the thinness of the films that had to be used in the experimental design.

14.4.2.2. *Randomized arrangements*

With regard to the simulations, it would be of considerable interest to investigate the reinforcing properties of such oblate particles when they are randomly oriented and also randomly dispersed. Such work is in progress [71].

14.5. Aggregated particles

14.5.1. *Real systems*

The silica or carbon black particles used to reinforce commercial materials are seldom completely dispersed [1–5], as is assumed in the simulations described. As is shown schematically in Figure 14.15, the primary particles are generally aggregated into relatively stable "aggregates" and these are frequently clustered into less-stable arrangements called "agglomerates" [40].

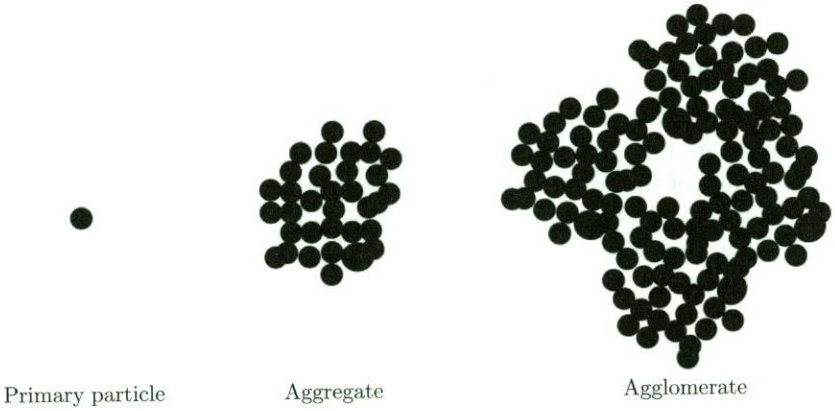

Figure 14.15. Sketches of primary particles, aggregates, and agglomerates occurring in fillers such as carbon black and silica

14.5.2. *Types of aggregates for modeling*

Simulations should be carried out on such more highly ordered structures, some limiting forms of which are sketched in Figure 14.16 [71]. It is well known in the industry that such structures are important in maximizing the reinforcement, as evidenced by the fact that being too persistent in removing such aggregates and agglomerates in blending procedures gives materials with less than optimal mechanical properties [1–5].

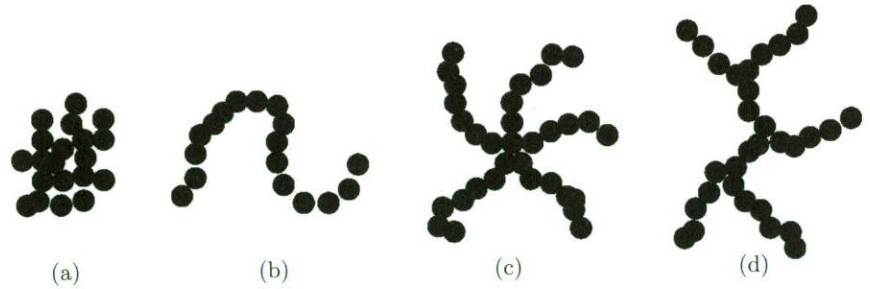

Figure 14.16. Four illustrative types of aggregates: (a) globular; (b) chainlike; (c) star-shaped; and (d) branched

14.5.3. *Deformabilities of aggregates*

Friedlander *et al.* have demonstrated that such aggregates have a remarkable deformability, by carrying out elongation experiments both reversibly, and irreversibly to their rupture points [99–104]. This is of considerable importance, since when these structures are within elastomeric matrices, their deformations upon deformation of the filled elastomer means that they must contribute to the storage of the elastic deformation energy. This would have to be taken into account both in the interpretation of experimental results and in more refined simulations of filler reinforcement.

14.6. Potential refinements

The characterized excluded volume effect is only one aspect of elastomer reinforcement [6–12], but some additional effects could be investigated by additional modeling of the adsorption of the elastomer chains onto the filler surface. The preliminary physisorption results described above should obviously be refined. Then, the calculations could be extended to include chemical adsorption by assuming that there are randomly-distributed, active particle sites interacting very strongly with the chains (by a Dirac δ-function type of potential). If the distance between the chain (generated using the Monte Carlo method) and the active site becomes less than the range of the short-range interactions, then the chain would become chemisorbed. The distribution of other active sites on the filler surface and the Lennard-Jones interactions would determine if the remaining parts of the chain are absorbed onto the surface. Simulations for chains sufficiently long to partially adsorb onto several filler particles would be especially illuminating, in that they could shed new light on the general problem of polymer adsorption. The distribution of the chain contours between the polymer bulk and various filler particles could also be of considerable importance.

14.7. Conclusions

Although there are obviously unresolved issues, the broad overview presented here should demonstrate the utility of simulations to give a better molecular understanding of how fillers reinforce elastomeric materials. It is also hoped that some of the unsolved problems described will encourage others to contribute to elucidating this important area of polymer science and engineering.

Acknowledgments

It is a pleasure to acknowledge the financial support provided J. E. Mark by the National Science Foundation through Grant DMR–0314760 (Polymers Program, Division of Materials Research). Also, A. Kloczkowski gratefully acknowledges the financial support provided by NIH grant 1R01GM072014-01.

References

1. Boonstra B B (1979) Role of Particulate Fillers in Elastomer Reinforcement: A Review, *Polymer* **20**:691–704.
2. Warrick E L, Pierce O R, Polmanteer K E and Saam J C (1979) Silicone Elastomer Developments 1967–1977, *Rubber Chem Technol* **52**:437–525.
3. Rigbi Z (1980) Reinforement of Rubber by Carbon Black, *Adv Polym Sci* **36**:21–68.
4. Donnet J-B and Vidal A (1986) Carbon Black: Surface Properties and Interactions with Elastomers, *Adv Polym Sci* **76**:103–127.
5. Donnet J and Custodero E (2005) Reinforcement of Elastomers by Particulate Fillers, in *Science and Technology of Rubber*, 3rd ed. (Eds. Mark J E and Erman B) Elsevier, Amsterdam, pp. 367–400.
6. Heinrich G and Vilgis T A (1993) Contribution of Entanglements to the Mechanical Properties of Carbon Black Filled Polymer Networks, *Macromolecules* **26**:1109–1119.
7. Witten T A, Rubinstein M and Colby R H (1993) Reinforcement of Rubber by Fractal Aggregates, *J Phys II France* **3**:367–383.
8. Kluppel M and Heinrich G (1995) Fractal Structures in Carbon Black Reinforced Rubbers, *Rubber Chem Technol* **68**:623–651.
9. Kluppel M, Schuster R H and Heinrich G (1997) Structure and Properties of Reinforcing Fractal Filler Networks in Elastomers, *Rubber Chem Technol* **70**:243–255.
10. Heinrich G, Kluppel M and Vilgis T A (2002) Reinforcement of Elastomers, *Curr Opinion Solid State Mats Sci* **6**:195–203.
11. Heinrich G and Kluppel M (2002) Recent Advances in the Theory of Filler Networking in Elastomers, *Adv Polym Sci* **160**:1–44.
12. Kluppel M (2003) The Role of Disorder in Filler Reinforcement of Elastomers on Various Length Scales, *Adv Polym Sci* **164**:1–86.
13. Kloczkowski A, Sharaf M A and Mark J E (1993) Molecular Theory for Reinforcement in Filled Elastomers, *Comput Polym Sci* **3**:39–45.
14. Sharaf M A, Kloczkowski A and Mark J E (1994) Simulations on the Reinforcement of Elastomeric Poly(Dimethylsiloxane) by Filler Particles Arranged on a Cubic Lattice, *Comput Polym Sci* **4**:29–39.
15. Kloczkowski A, Sharaf M A and Mark J E (1994) Computer Simulations on Filled Elastomeric Materials, *Chem Eng Sci* **49**:2889–2897.
16. Yuan Q W, Kloczkowski A, Mark J E and Sharaf M A (1996) Simulations on the Reinforcement of Poly(dimethylsiloxane) Elastomers by Randomly-Distributed Filler Particles, *J Polym Sci, Polym Phys Ed* **34**:1647–1657.
17. Hooper J B, McCoy J D and Curro J G (2000) Density Functional Theory of Simple Polymers in a Slit Pore. I. Theory and Efficient Algorithm, *J Chem Phys* **112**:3090–3093.
18. Vacatello M (2001) Monte Carlo Simulations of Polymer Melts Filled with Solid Nanoparticles, *Macromolecules* **34**:1946–1952.
19. Sharaf M A, Kloczkowski A and Mark J E (2001) Monte Carlo Simulations on Reinforcement of an Elastomer by Oriented Prolate Particles, *Comput Theor Polym Sci* **11**:251–262.
20. Sharaf M A and Mark J E (2002) Monte Carlo Simulations on Filler-Induced Network Chain Deformations and Elastomer Reinforcement from Oriented Oblate Particles, *Polymer* **43**:643–652.
21. Vacatello M (2002) Molecular Arrangements in Polymer-Based Nanocomposites, *Macromol Theor Sims* **11**:757–765.

22. Gersappe D (2002) Molecular Mechanisms of Failure in Polymer Nanocomposites, *Phys Rev Lett* **89**:58301–58304.
23. Fuchs M and Schweizer K S (2002) Structure of Colloid-Polymer Suspensions, *J Phys Conden Mat* **14**:R239–269.
24. Vacatello M (2002) Chain Dimensions in Filled Polymers: An Intriguing Problem, *Macromolecules* **35**:8191–8193.
25. Ozmusul M S and Picu R C (2002) Structure of Polymers in the Vicinity of Convex Impenetrable Surfaces: The Athermal Case, *Polymer* **43**:4657–4665.
26. Picu R C and Ozmusul M S (2002) Structure of Linear Polymeric Chains Confined Between Impenetrable Spherical Walls, *J Chem Phys* **118**:11239–11248.
27. Starr F W, Schroeder T B and Glotzer S C (2002) Molecular Dynamics Simulation of a Polymer Melt with a Nanoscopic Particle, *Macromolecules* **35**:4481–4492.
28. Mark J E (2002) Some Simulations on Filler Reinforcement in Elastomers, *Molec Cryst Liq Cryst* **374**:29–38.
29. Schmidt G and Malwitz M M (2003) Filler Simulations, *Curr Opinion Coll Interfac Sci* **8**:103–108.
30. Vacatello M (2003) Phantom Chain Simulations of Polymer-Nanofiller Simulations, *Macromolecules* **36**:3411–3416.
31. Vacatello M (2003) Predicting the Molecular Arrangements in Polymer-Based Nanocomposites, *Macromol Theor Sims* **12**:86–91.
32. Hooper J B, Schweizer K S, Desai T G, Koshy R and Keblinski P (2004) Structure, Surface Excess and Effective Interactions in Polymer Nanocomposite Melts and Concentrated Solutions, *J Chem Phys* **121**:6986–6997.
33. Vacatello M (2004) Monte Carlo Simulations of Polymers in Nanoslits, *Macromol Theor Sims* **13**:30–35.
34. Barbier D, Brown D, Grillet A C and Neyertz S (2004) Interface between End-Functionalized PEO Oligomers and a Silica Nanoparticle Studied by Molecular Dynamics Simulations *Macromolecules* **37**:4695–4710.
35. Sharaf M A and Mark J E (2004) Monte Carlo Simulations on the Effects of Nanoparticles on Chain Deformations and Reinforcement in Amorphous Polyethylene Networks, *Polymer* **45**:3943–3952.
36. Doxastakis M, Chen Y L, Guzman O and de Pablo J J (2004) Polymer-Particle Mixtures: Depletion and Packing Effects, *J Chem Phys* **120**:9335–9342.
37. Lin H and Mattice W L (2004) Monte Carlo Simulations of the Chain Dimensions in Filled Polyethylene Melts, Abstracts, *POLY Workshop on Molecular Modeling of Macromolecules*, Hilton Head, 2004:10.
38. Vacatello M and Vacatello M (2005) Molecular Arrangements in Polymer Nanofiller Systems, in *Computer Simulations of Liquid Crystals and Polymers* (Eds. Pasini P, Zannoni C and Zumer S) Kluwer Academic Publishers, Dordrecht, pp. 109–133.
39. Ozmusul M S, Picu R C, Sternstein S S and Kumar S K (2005) Lattice Monte Carlo Simulations of Chain Conformations in Polymer Nanocomposites, *Macromolecules* **38**:4495–4500.
40. Mark J E, Abou-Hussein R, Sen T Z and Kloczkowski A (2005) Some Simulations on Filler Reinforcement of Elastomers, *Polymer* **46**:8894–8904.
41. Sen T Z, Sharaf M A, Mark J E and Kloczkowski A (2005) Modeling the Elastomeric Properties of Stereoregular Polypropylenes in Nanocomposites with Spherical Fillers, *Polymer* **46**:7301–7308.
42. Sharaf M A, Kloczkowski A, Sen T Z, Jacob K I and Mark J E (2006) Molecular Modeling of Matrix Chain Deformation in Nanofiber Filled Composites, *Colloid Polymer Sci* **284**:700–709.

43. Sharaf M A, Kloczkowski A, Sen T Z, Jacob K I and Mark J E (2006) Filler-Induced Deformations of Amorphous Polyethylene Chains. The Effects of the Deformations on Elastomeric Properties, and Some Comparisons with Experiment, *Eur Polym J* **42**:796–806.
44. Mark J E, Abou-Hussein R, Sen T Z and Kloczkowski A (2007) Monte Carlo Simulations on Nanoparticles in Elastomers. Effects of the Particles on the Dimensions of the Polymer Chains and the Mechanical Properties of the Networks, *Macromol Symp* **256**:40–47.
45. Sen S, Thomin J D, Kumar S K and Keblinski P (2007) Molecular Underpinnings of the Mechanical Reinforcement in Polymer Nanocomposites, *Macromolecules* **40**:4059–4067.
46. Wu S and Mark J E (2007) Some Simulations and Theoretical Studies on Poly(dimethylsiloxane), *J Macrom Sci, Polym Revs* **47**:463–485.
47. Flory P J (1969) *Statistical Mechanics of Chain Molecules*, Interscience, New York.
48. Mattice W L and Suter U W (1994) *Conformational Theory of Large Molecules. The Rotational Isomeric State Model in Macromolecular Systems*, Wiley, New York.
49. Rehahn M, Mattice W L and Suter U W (1997) Rotational Isomeric State Models in Macromolecular Systems, *Adv Polym Sci* **131/132**:1–18.
50. Flory P J (1953) *Principles of Polymer Chemistry*, Cornell University Press, Ithaca NY.
51. Mark J E and Curro J G (1983) A Non-Gaussian Theory of Rubberlike Elasticity Based on Rotational Isomeric State Simulations of Network Chain Configurations. I. Polyethylene and Polydimethylsiloxane Short-Chain Unimodal Networks, *J Chem Phys* **79**:5705–5709.
52. DeBolt L C and Mark J E (1988) Theoretical Stress-Strain Isotherms for Elastin Model Networks, *J Polym Sci, Polym Phys Ed* **26**:865–874.
53. Mark J E and Curro J G (1984) A Non-Gaussian Theory of Rubberlike Elasticity Based on Rotational Isomeric State Simulations of Network Chain Configurations. III. Networks Prepared from the Extraordinarily Flexible Chains of Polymeric Sulfur and Polymeric Selenium, *J Chem Phys* **80**:5262–5265.
54. Treloar L R G (1975) *The Physics of Rubber Elasticity*, 3rd ed., Clarendon Press, Oxford.
55. Mark J E (2003) Some Recent Theory, Experiments, and Simulations on Rubberlike Elasticity, *J Phys Chem, Part B* **107**:903–913.
56. Mark J E and Erman B (2007) *Rubberlike Elasticity. A Molecular Primer*, 2nd ed., Cambridge University Press, Cambridge.
57. Erman B and Mark J E (1997) *Structures and Properties of Rubberlike Networks*, Oxford University Press, New York.
58. Mark J E (2003) Elastomers with Multimodal Distributions of Network Chain Lengths, *Macromol Symp, St. Petersburg issue* **191**:121–130.
59. Mark J E (2004) Some Interesting Things About Polysiloxanes, *Acct Chem Res* **37**:946–953.
60. Sunkara H B, Jethmalani J M and Ford W T (1994) Composite of Colloidal Crystals of Silica in Poly(methyl methacrylate), *Chem Mater* **6**:362–364.
61. Sunkara H B, Jethmalani J M and Ford W T (1995) Solidification of Colloidal Crystals of Silica, in *Hybrid Organic-Inorganic Composites* (Eds. Mark J E, Lee C Y-C and Bianconi P A) American Chemical Society, Washington, Vol. 585, pp. 181–191.
62. Pu Z, Mark J E, Jethmalani J M and Ford W T (1996) Mechanical Properties of a Poly(methyl acrylate) Nanocomposite Containing Regularly-Arranged Silica Particles, *Polym Bull* **37**:545–551.

63. Pu Z, Mark J E, Jethmalani J M and Ford W T (1997) Effects of Dispersion and Aggregation of Silica in the Reinforcement of Poly(methyl acrylate) Elastomers, *Chem Mater* **9**:2442–2447.
64. Nakatani A I, Chen W, Schmidt R G, Gordon G V and Han C C (2001) Chain Dimensions in Polysilicate-Filled Poly(Dimethylsiloxane), *Polymer* **42**:3713–3722.
65. Nakatani A I, Chen W, Schmidt R G, Gordon G V and Han C C (2002) Chain Dimensions in Polysilicate-Filled Poly(Dimethylsiloxane), *Int J Thermophys* **23**:199–209.
66. Mackay M E, Tuteja A, Duxbury P M, Hawker C J, Horn B V, Guan Z, Chen G and Krishnan R S (2006) General Strategies for Nanoparticle Dispersion, *Science* **311**:1740–1743.
67. Huang J, Mao Z and Qian C (2006) Dynamic Monte Carlo Study on the Polymer Chain in Random Media Filled with Nanoparticles, *Polymer* **47**:2928–2932.
68. Erguney F M, Lin H and Mattice W L (2006) Dimensions of Matrix Chains in Polymers Filled with Energetically Neutral Nanoparticles, *Polymer* **47**:3689–3695.
69. Erguney F M and Mattice W L, Response of Matrix Chains to Nanoscale Filler Particles, *Polymer* (submitted).
70. Sen T Z and Kloczkowski A (unpublished results).
71. Abou-Hussein R and Mark J E (unpublished results).
72. Holmes G A and Letton A (1994) Bisphenol-A Bimodal Epoxy Resins. Part I: The Dynamic Mechanical Characterization of a 6300 (340/22,500) Weight Average Molecular Weight System, *Polym Eng Sci* **34**:1635–1642.
73. Okamoto Y, Miyagi H, Kakugo M and Takahashi K (1991) Impact Improvement Mechanism of HIPS with Bimodal Distribution of Rubber Particle Size, *Macromolecules* **24**:5639–5644.
74. Chen T K and Jan Y H (1992) Fracture Mechanism of Toughened Epoxy Resin with Bimodal Rubber-Particle Size Distribution, *J Mater Sci* **27**:111–121.
75. Takahashi J, Watanabe H, Nakamoto J, Arakawa K and Todo M (2006) In-Situ Polymerization and Properties of Methyl Methacrylate-Butadiene-Styrene Resin with Bimodal Rubber Particle Size Distributions, *Polym J* **38**:835–843.
76. Premachandra J and Mark J E (2002) Effects of Dilution During Cross Linking on Strain-Induced Crystallization in *cis*-1,4-Polyisoprene Networks. 1. Experimental Results, *J Macromol Sci, Pure Appl Chem* **39**:287–300.
77. Premachandra J, Kumudinie C and Mark J E (2002) Effects of Dilution During Cross Linking on Strain-Induced Crystallization in *cis*-1,4-Polyisoprene Networks. 2. Comparison of Experimental Results with Theory, *J Macromol Sci, Pure Appl Chem* **39**:301–320.
78. Urayama K and Kohjiya S (1997) Uniaxial Elongation of Deswollen Polydimethylsiloxane Networks with Supercoiled Structure, *Polymer* **38**:955–962.
79. Kohjiya S, Urayama K and Ikeda Y (1997) Poly(Siloxane) Network of Ultra-High Elongation, *Kautschuk Gummi Kunststoffe* **50**:868–872.
80. Urayama K and Kohjiya S (1998) Extensive Stretch of Polysiloxane Network Chains with Random- and Super-Coiled Conformations, *Eur Phys J B* **2**:75–78.
81. Kloczkowski A, Sen T Z and Sharaf M A (2005) The Largest Eigenvalue Method for Stereo-Regular Vinyl Chains, *Polymer* **46**:4373–4383.
82. Erman B and Mark J E (2005) The Molecular Basis of Rubberlike Elasticity, in *Science and Technology of Rubber*, 3rd ed. (Eds. Mark J E, Erman B and Eirich F R) Academic, San Diego, pp. 157–182.
83. Medalia A I and Kraus G (1994) Reinforcement of Elastomers by Particulate Fillers, in *Science and Technology of Rubber*, 2nd ed. (Eds. Mark J E, Erman B and Eirich F R) Academic, San Diego, pp. 387–418.

84. Fried J R (2003) *Polymer Science and Technology*, 2nd ed., Prentice Hall, Englewood Cliffs, NJ.
85. Okada A, Kawasumi M, Usuki A, Kojima Y, Kurauchi T and Kamigaito O (1990) Nylon 6-Clay Hybrid, in *Polymer-Based Molecular Composites* (Eds. Schaefer D W and Mark J E) Materials Research Society, Pittsburgh, Vol. 171, pp. 45–50.
86. Pinnavaia T J, Lan T, Wang Z, Shi H and Kaviratna P D (1996) Clay-Reinforced Epoxy Nanocomposites: Synthesis, Properties, and Mechanism of Formation, in *Nanotechnology. Molecularly Designed Materials* (Eds. Chow G-M and Gonsalves K E) American Chemical Society, Washington, Vol. 622, pp. 250–261.
87. Giannelis E P (1996) Organoceramic Nanocomposites, in *Biomimetic Materials Chemistry* (Ed. Mann S) VCH Publishers, New York, pp. 337–59.
88. Vaia R A and Giannelis E P (2001) Liquid Crystal Polymer Nanocomposites: Direct Intercalation of Thermotropic Liquid Crystalline Polymers into Layered Silicates, *Polymer* **42**:1281–1285.
89. Pinnavaia T J and Beall G (Eds.) (2001) *Polymer-Clay Nanocomposites*, Wiley, New York.
90. Auerbach S M, Carrado K A and Dutta P B (Eds.) (2004) *Handbook of Layered Materials*, Marcel Dekker, New York.
91. Fischer H (2003) Polymer Nanocomposites: From Fundamental Research to Specific Applications, *Mat Sci Engin, C* **23**:763–772.
92. Ray S S and Okamoto M (2003) Polymer/Layered Silicate Nanocomposites: A Review from Preparation to Processing, *Prog Polym Sci* **28**:1539–1641.
93. Ahmadi S J, Huang Y D and Li W (2004) Synthetic Routes, Properties and Future Applications of Polymer-Layered Silicate Nanocomposites, *J Mater Sci* **39**:1919–1925.
94. Kawasumi M (2004) The Discovery of Polymer-Clay Hybrids, *J Polym Sci, Polym Chem Ed* **42**:819–824.
95. Usuki A, Hasegawa N and Kato M (2005) Polymer-Clay Nanocomposites, *Adv Polym Sci* **179**:135–195.
96. Zhu J and Wilkie C A (2007) Inercalation Compounds and Clay Nanocomposites, in *Hybrid Materials. Synthesis, Characterization, and Applications* (Ed. Kickelbick G) Wiley-VCH Verlag, Weinheim, pp. 151–173.
97. Wang S and Mark J E (1990) Generation of Glassy Ellipsoidal Particles within an Elastomer by In-situ Polymerization, Elongation at an Elevated Temperature, and Finally Cooling Under Strain, *Macromolecules* **23**:4288–4291.
98. Wang S, Xu P and Mark J E (1991) Method for Generating Oriented Oblate Ellipsoidal Particles in an Elastomer and Characterization of the Reinforcement They Provide, *Macromolecules* **24**:6037–6039.
99. Ogawa K, Vogt T, Ullmann M, Johnson S and Friedlander S K (2000) Elastic Properties of Nanoparticle Chain Aggregates of TiO_2, Al_2O_3, and Fe_2O_3 Generated by Laser Ablation, *J Appl Phys* **87**:63–73.
100. Suh Y J, Ullmann M, Friedlander S K and Park K Y (2001) Elastic Behavior of Nanoparticle Chain Aggregates (NCA): Effects of Substrate on NCA Stretching and First Observations by a High-Speed Camera, *J Phys Chem B* **105**:11796–11799.
101. Friedlander S K, Jang H D and Ryu K H (1998) Elastic Behavior of Nanoparticle Chain Aggregates, *Appl Phys Lett* **72**:11796–11799.
102. Suh Y J, Prikhodko S V and Friedlander S K (2002) Nanostructure Manipulation Device for Transmission Electron Microscopy: Application to Titania Nanoparticle Chain Aggregates, *Microsc Microanal* **8**:497–501.

103. Suh Y J and Friedlander S K (2003) Origin of the Elastic Behavior of Nanoparticle Chain Aggregates: Measurements Using Nanostructure Manipulation Device, *J Appl Phys* **93**:3515–3523.
104. Rong W, Pelling A E, Ryan A, Gimzewski J K and Friedlander S K (2004) Complementary TEM and AFM Force Spectroscopy to Characterize the Nanomechanical Properties of Nanoparticle Chain Aggregates, *Nano Lett* **4**:2287–2292.